



Tenth U.S. National Conference on Earthquake Engineering
Frontiers of Earthquake Engineering
July 21-25, 2014
Anchorage, Alaska

WHAT HAVE WE LEARNED AFTER A DECADE OF EXPERIMENTS AND MONITORING AT THE NEES@UCSB PERMANENTLY INSTRUMENTED FIELD SITES?

Jamison H. Steidl¹, Francesco Civilini², and Sandra Seale³

ABSTRACT

New observations of pore pressure and acceleration with depth are providing *in situ* empirical evidence documenting the range of ground motion and dynamic strain levels at which the onset of nonlinear behavior and excess pore pressure begins, augmenting previous case history data, and cyclic tri-axial and centrifuge laboratory testing. The largest static pore pressure increases observed in the “NEES” decade of monitoring were generated by four events at the Wildlife Liquefaction Array (WLA) site, ranging in magnitude from 4.6 to 5.4 and all at distances less than 10 km from the site. The largest peak horizontal acceleration of ~ 325 gals was generated by a M4.9 event. This event generated ~ 20 kPa of excess pore pressure on multiple transducers, with a pore pressure ratio R_u of $\sim 60\%$ near the top of the liquefiable layer. Peak strain levels reached as high as 1.8×10^{-3} . The excess pore pressure can be seen migrating from the top of the layer towards the bottom, as well as dissipation that can take hours, highlighting the importance of continuous monitoring instead of triggered. Nonlinear soil behavior is analyzed in terms of changes in travel times (decrease in shear wave velocity) between accelerometers in the array for the largest ground motions, as well as a reduction in high frequency amplification. Analysis of data during the largest excitation at the site show that the nonlinear soil behavior occurs both near the surface and even at depths greater than 30 meters. The soil is observed to recover its pre-event low-strain velocities quickly following these larger events.

¹Research Professor, Earth Research Institute, University of California, Santa Barbara, CA 93106-1100

²Graduate Student, Earth Research Institute, University of California, Santa Barbara, CA 93106-1100

³Associate Project Scientist, Earth Research Institute, University of California, Santa Barbara, CA 93106-1100



Tenth U.S. National Conference on Earthquake Engineering
Frontiers of Earthquake Engineering
July 21-25, 2014
Anchorage, Alaska

WHAT HAVE WE LEARNED AFTER A DECADE OF EXPERIMENTS AND MONITORING AT THE NEES@UCSB PERMANENTLY INSTRUMENTED FIELD SITES?

Jamison H. Steidl¹, Francesco Civilini², and Sandra Seale³

ABSTRACT

New observations of pore pressure and acceleration with depth are providing in situ empirical evidence documenting the range of ground motion and dynamic strain levels at which the onset of nonlinear behavior and excess pore pressure begins, augmenting previous case history data, and cyclic tri-axial and centrifuge laboratory testing. The largest static pore pressure increases observed in the “NEES” decade of monitoring were generated by four events at the Wildlife Liquefaction Array (WLA) site, ranging in magnitude from 4.6 to 5.4 and all at distances less than 10 km from the site. The largest peak horizontal acceleration of ~325 gals was generated by a M4.9 event. This event generated ~20 kPa of excess pore pressure on multiple transducers, with a pore pressure ratio R_u of ~60% near the top of the liquefiable layer. Peak strain levels reached as high as 1.8×10^{-3} . The excess pore pressure can be seen migrating from the top of the layer towards the bottom, as well as dissipation that can take hours, highlighting the importance of continuous monitoring instead of triggered. Nonlinear soil behavior is analyzed in terms of changes in travel times (decrease in shear wave velocity) between accelerometers in the array for the largest ground motions, as well as a reduction in high frequency amplification. Analysis of data during the largest excitation at the site show that the nonlinear soil behavior occurs both near the surface and even at depths greater than 30 meters. The soil is observed to recover its pre-event low-strain velocities quickly following these larger events.

Introduction

A goal of engineering seismology geotechnical earthquake engineering research is to generate analytical and empirical models for accurate prediction of ground shaking, excess pore water pressure generation, ground deformation, and soil-foundation-structure interaction (SFSI). The development of simulation capabilities that can reproduce these effects at various strain levels requires well-instrumented test sites where actual ground response, pore pressure, and deformation can be monitored during earthquake shaking to provide benchmark case histories for verification of the simulation models. The University of California at Santa Barbara (UCSB) operates one of the 14 earthquake engineering experimental facilities that are part of the US National Science Foundation (NSF) George E. Brown, Jr., Network for Earthquake Engineering

¹Research Professor, Earth Research Institute, University of California, Santa Barbara, CA 93106-1100

²Graduate Student, Earth Research Institute, University of California, Santa Barbara, CA 93106-1100

³Associate Project Scientist, Earth Research Institute, University of California, Santa Barbara, CA 93106-1100

Simulation (NEES) Program. The NEES@UCSB facility includes the Wildlife Liquefaction Array (WLA) and Garner Valley Downhole Array (GVDA) located in southern California. These densely instrumented geotechnical and structural engineering field sites continuously record both acceleration and pore pressure. Accelerometers are located on the surface and at various depths below the surface, and pore pressure transducers are installed at depth within the liquefiable layers. Permanently instrumented structures for examining soil-foundation-structure interaction (SFSI), and a permanent cross-hole array, have transformed these sites into multi-disciplinary earthquake engineering research facilities [1,2,3,4,5].

Over the last decade, local and regional seismic activity, including multiple extremely active earthquake swarms, have produced a valuable new data set providing a unique opportunity to observe site response and the evolution of pore pressure generation with time throughout the liquefiable layer, and at an unprecedented level of detail. In addition to the earthquakes provided by nature, active testing experiments using the mobile shakers from NEES@UTexas and NEES@UCLA have produced an equally valuable data set on both site characterization studies and soil-foundation-structure interaction. Due to limitations in the length of contributions to the 10NCEE, this manuscript focuses on recent observations at the WLA site.

The Wildlife Liquefaction Array (WLA) is located on the west bank of the Alamo River 13 km due north of Brawley, California and 160 km due east of San Diego. The site is located in the Imperial Wildlife Area, a California State game refuge. Earthquakes have frequently shaken this region, with six in the past 75 years generating liquefaction effects at or within 10 km of the WLA site [2]. Based on this history, there is high expectation that additional liquefaction-producing earthquakes will shake the WLA site in the future, which led to the selection of this location for development of a permanently instrumented facility. Fig. 1 is a view of the WLA site after construction was completed in Fall 2004. Details of the geotechnical site conditions and instrumentation at the WLA facility can be found at the NEES@UCSB website (<http://nees.ucsb.edu/>), and in previous studies of the observations from this site [4,6,7,8,9]. Data from the sensors at the WLA site shown in Fig. 2 are recorded continuously and transmitted back to UCSB via the High Performance Wireless Research and Education Network (HPWREN) via UC San Diego. Earthquake data recorded at WLA are segmented out from the continuous data using the earthquake catalog provided by the Southern California Seismic Network (SCSN: <http://www.scsn.org/>), part of the California Integrated Seismic Network (<http://www.cisn.org>) and the Advanced National Seismic System (<http://earthquake.usgs.gov/monitoring/anss/>). This event data is processed and made available to the public via the NEES@UCSB data dissemination portal (<http://www.nees.ucsb.edu/data-portal>).



Figure 1. Panoramic view of the NEES WLA facility during site visit in February 2013.

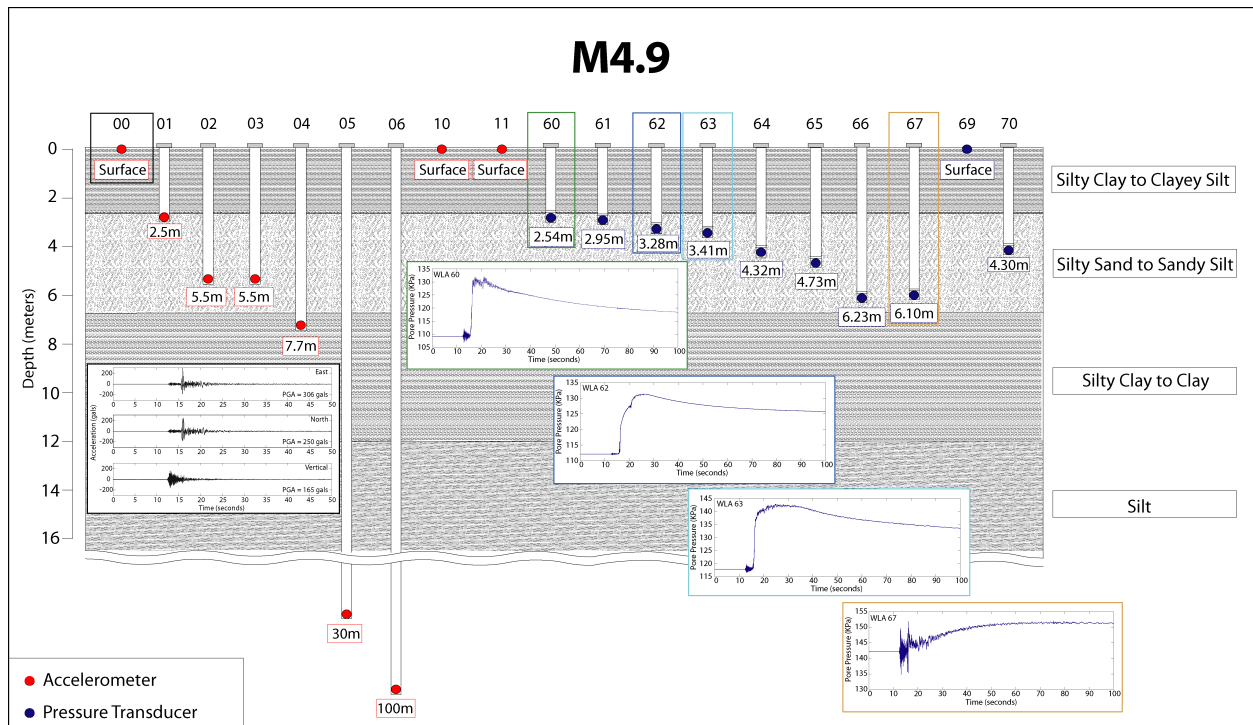


Figure 2. Cross-section of acceleration and pore pressure instrumentation at the WLA site. Inset images show selected data from the 27 August 2012 M4.9 earthquake and are color coded to the box surrounding the sensor they correspond to.

WLA Observations of the 2012 Brawley Swarm

The 2012 Brawley swarm started near the town of Brawley at 4h30m (GMT) on 26 August, with over 600 events being located by the SCSN during this swarm [10]. At the WLA site, where continuous data is transmitted back to UCSB and archived, six events produced significant ground motions ($>1 \text{ m/s}^2$). The continuous data from a the East-West component of surface acceleration is shown in Fig. 3 for a 16 hour time period during the largest events in the swarm. Each acceleration channel and pore pressure channel at the WLA site is recorded at 200 samples per second, continuously, providing the opportunity to examine how the soil responds to repeated shaking. In addition, with continuous pore pressure observations, we can examine with high spatial and temporal resolution, how excess pore pressure is generated and dissipated with time, throughout the repeated shaking during the swarm.

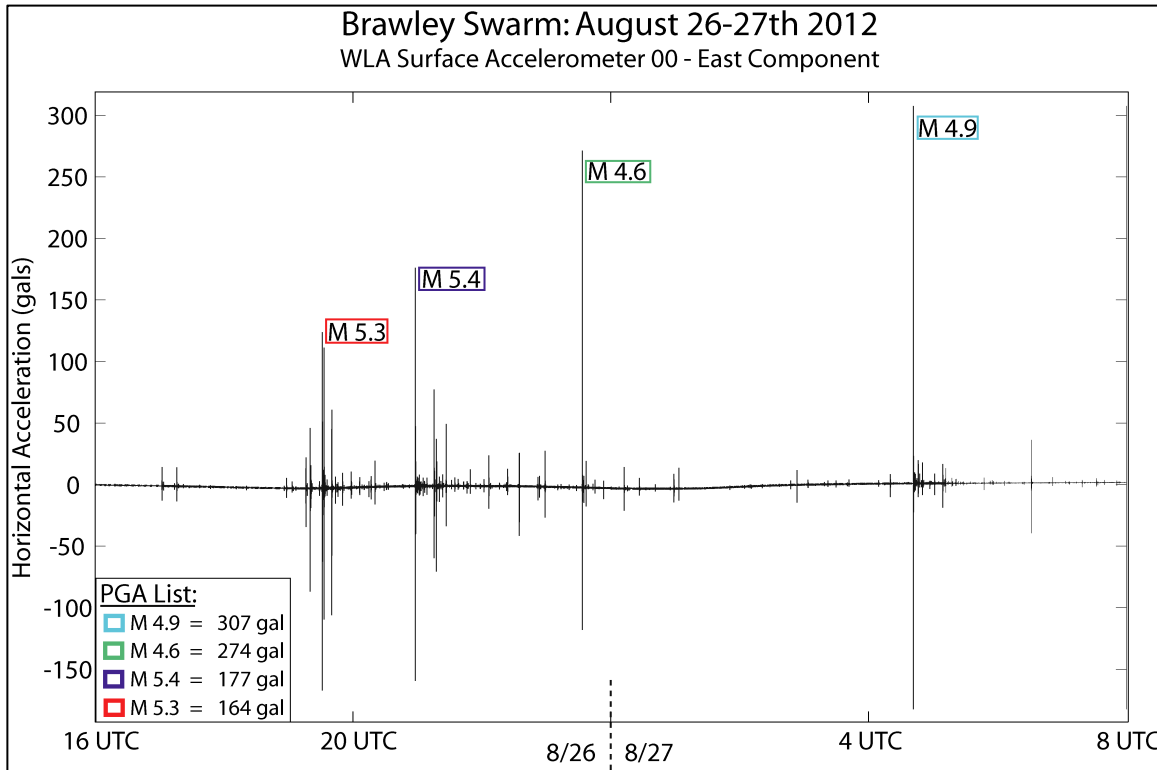


Figure 3. Sixteen hours of continuous acceleration data from the East component recorded at the surface of the WLA site. The four largest events are highlighted, with the peak accelerations listed in the lower left corner.

Analysis and Results

The Brawley swarm provides an unprecedented data set of pore pressure and acceleration data recorded within and surrounding the liquefiable layer at the WLA site. Admittedly, events of this magnitude would not necessarily be considered significant in terms of adding to the number of case histories used for the determining liquefaction resistance of soils [11]. However, they do provide extremely interesting insights into the details of the physics of excess pore pressure generation, and the liquefaction process. These *insitu* details augment the data from laboratory and centrifuge test, and enable our theoretical simulation capabilities and constitutive models to be validated against field case history data.

Nonlinear Soil Behavior: Reduction in High Frequency

One simple way to use vertical array data to examine dynamic soil behavior and nonlinearity with increasing shaking level is to look at the ratio of ground motions recorded at the surface relative to at depth. The simplest case is to look at the ratio of peak acceleration, which for near source earthquakes is typically in the high frequency part of the spectrum. We use the ration of the peak acceleration at the surface relative to the 100-meter borehole sensor, and plot this ratio versus the surface peak acceleration. It is expected that this simple measure of site amplification would tend to decrease with increasing ground shaking due to the softening of the soil and increased damping. Fig. 4 shows these ratios for M3.0 events and larger, during the Brawley Swarm. The events with lower levels of shaking, while having some variability, cluster around

what is the nominal high frequency amplification for the WLA site, while the events with larger levels of shaking show lower amplification levels, evidence of nonlinear soil behavior.

Nonlinear Soil Behavior: Reduction in S-wave velocity

Another way to examine dynamic soil behavior is through changes in shear-wave velocities as ground shaking increases. It is expected that shear modulus degradation will occur during significant shaking ($> 1 \text{ m/s}^2$), or increase strain levels, and this softening of the site will then cause the shear-wave velocity to decrease. We use the same set of events used in Fig. 4, and use cross-correlation between 100-meter and surface S-wave arrivals, to calculate the correlation lag, which given the distance between sensors, provides the interval velocity between sensors.

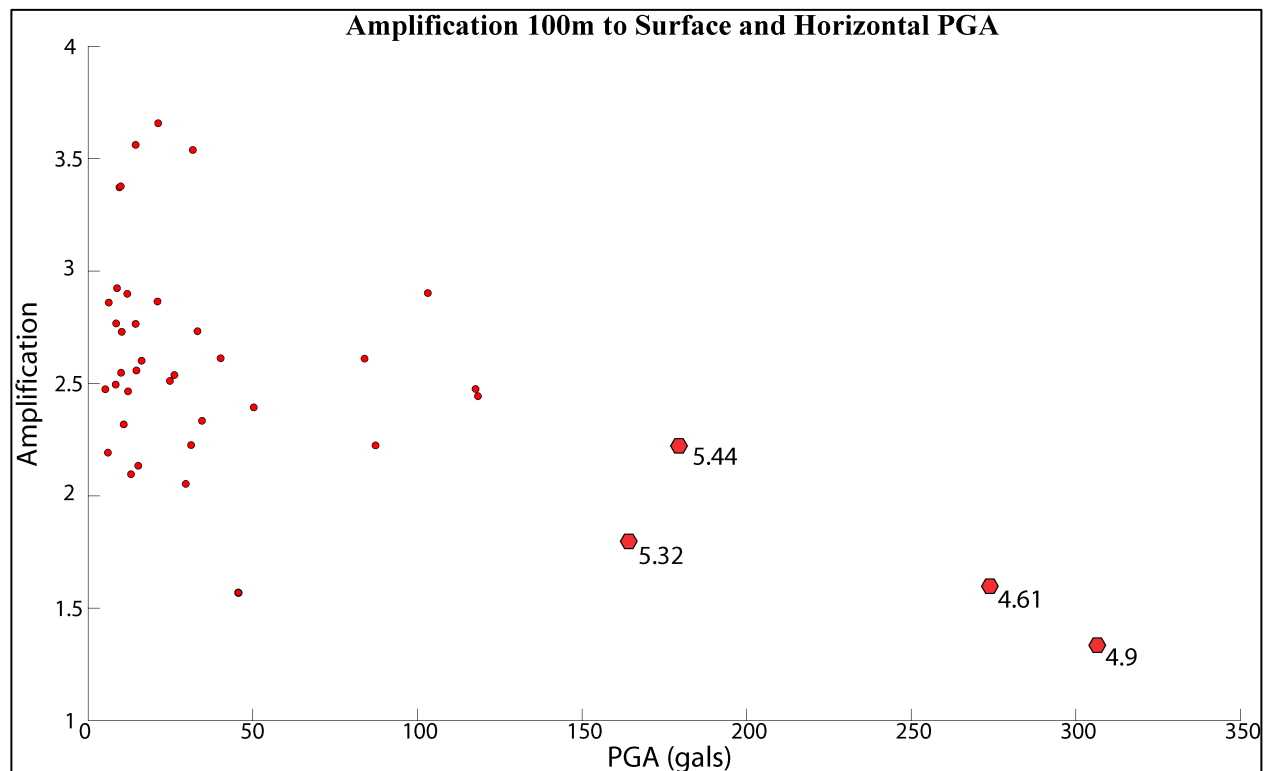


Figure 4. Ratio of peak acceleration at surface to 100 meter borehole plotted versus peak surface acceleration (cm/s^2) for 46 events with $M > 3.0$ in the Brawley swarm (shown in red). The four larger events are shown with large hexagonal symbols with earthquake magnitude annotated to the right.

Fig. 5a is a plot of this time lag plotted versus peak surface ground acceleration. The smaller events, which occur both before and after the larger events, tend to show some variability around the nominal correlation lag (velocity) at the WLA site between these sensors (similar to Fig. 4 results). As the surface ground shaking increases, the correlation lag increases. This increase in time lag of the S-wave pulse traveling from 100 meters to the surface, with increasing ground motion level, indicates that shear modulus degradation has decreased the S-wave velocity, somewhere in the upper 100 meters. This decrease represents a $\sim 10\%$ change in V_s from 100 meters to the surface for the M4.9 event. Interval velocity calculated from the correlation lag is shown on the right axis of the Fig. 5 for comparison.

The density of accelerometers in the soil column at the WLA site provides the opportunity to examine in finer detail where this nonlinearity is occurring. In Fig. 5b the cross-correlations between the 30-meter sensor and the surface are shown, for the same set of events. In this case the decrease in velocity represents a $\sim 17\%$ decrease in V_s , or a G/G_{\max} of ~ 0.8 (assuming density is not changing). In Fig. 5c the results are plotted for the 7.7-meter and surface sensors. In this case we can see that the largest ground shaking during the M4.9 event causes the velocity to decrease from ~ 135 m/s to ~ 100 m/s, a $\sim 30\%$ decrease in V_s , or a G/G_{\max} of 0.7. While not unexpected considering the soft liquefiable layer that exists in the upper 7.7 meters at the WLA site (Fig. 2), it is interesting to note that there is still nonlinearity occurring deeper in the soil layer. Fig. 5d shows the results using the 100-meter to 30-meter borehole sensors. Even deeper in the soil profile, we can see a $\sim 5\%$ change in velocity related to the larger ground motions from the M4.9 event.

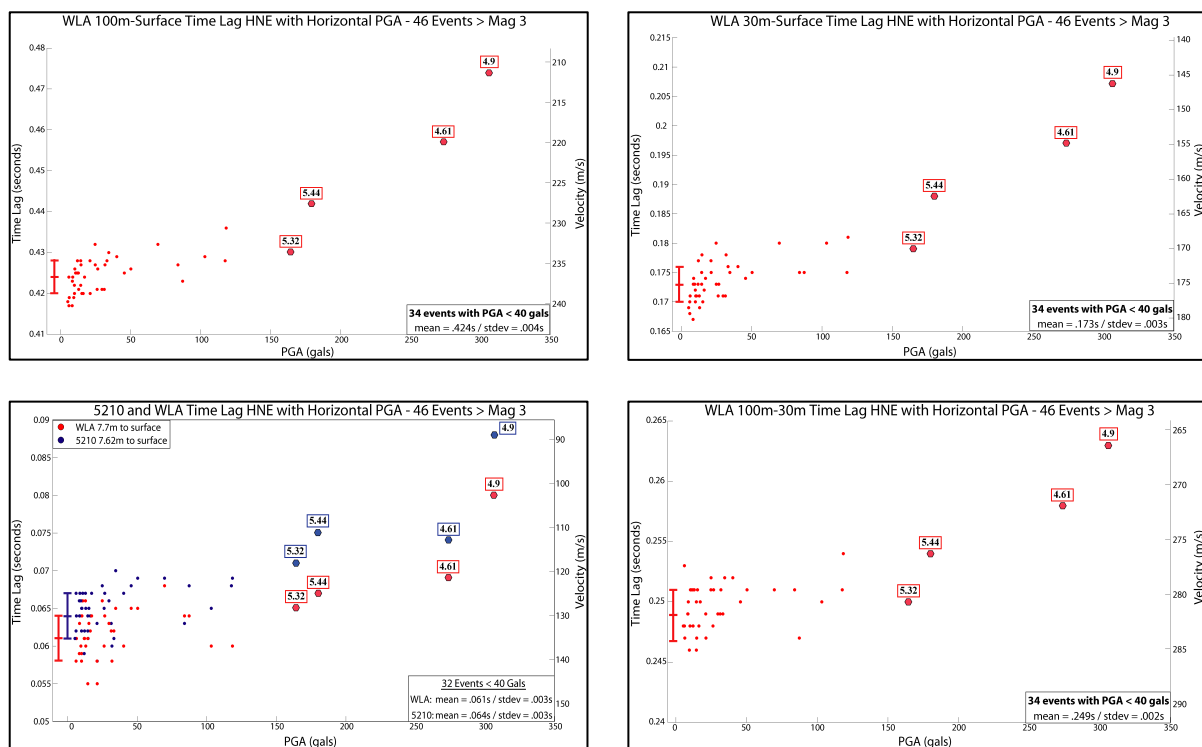


Figure 5. Cross-Correlation time lag plotted versus surface PGA at WLA site. (5a - Top Left): 100-meter to surface. (5b - Top Right): 30-meter to surface. (5c – Lower Left): 7.7-meter to surface at WLA (red) and 7.6-meter to surface at 1982 WLA site (blue). (5d – Lower Right): 100-meter to 30-meter.

Excess Pore Pressure Generation vs. PGA and Strain

The combination of good analog pressure sensor technology with high-resolution data acquisition systems have provided a unique opportunity to examine the initiation of excess pore pressure generation through earthquake observations at the NEES@UCSB sites. We measure pressure in isolation at various depths within the liquefiable layer (Fig. 2). These measurements are typically expressed in kilo-Pascal (kPa), or pore pressure ratio R_u , a value between 0% and 100%, in which an R_u of 0% represents the normal hydrostatic pressure level, and 100% represents a pressure level equal to the lithostatic load (weight of the soil above the sensor

depth), a level at which the site would be considered liquefied. Many small events are seen to cause a dynamic change in pore pressure resulting from seismic wave oscillations passing the site, but fewer events cause an observable step increase in pressure. In particular, measurements from the Brawley swarm have doubled the dataset of events that cause a static excess pore pressure increase. Many of these events have excess pressure generation of less than 0.1 kPa, and some as small as 0.01 kPa. Still, these are detectable static steps even at this small level.

An example of excess pore pressure generation can clearly be seen in the data shown on Fig. 2. This is an example where the excess pore pressure is more than 20 kPa near the surface of the liquefiable layer, and reaches an R_u of greater than 60%. These observations also show that the pressure at WLA tends to increase the most near the top of the liquefiable layer, just below the impermeable clay cap. The continuous data shows that the dissipation of excess pressure tends to be downward through the layer. While the pressure near the top of the layer begins to dissipate, the pressure is increasing towards the middle and bottom of the layer, showing the migration of the pressure pulse away from the base of the clay layer. Close examination of the pressure observations in Fig. 2 show sensor 67 is still increasing at 60 seconds after the event, while the sensors near the top of the layer (60, 62, 63) are dissipating.

In looking at the data set of 46 $M > 3.0$ events from the Brawley swarm, we find that 18 events generated an excess pore pressure step, two of these accompanied by significant excess pore pressure generation ($R_u > 50\%$) the other two with moderate excess pore pressure generation ($R_u > 10\%$). In 11 cases, the excess pore pressure generation occurs in the wake of a previous event, causing a ratcheting up of the excess pore pressure before it continues to dissipate. We call these events “coda” events, and will differentiate these from the other “jump” events when plotting excess pore pressure ratio versus ground motion level or strain.

In Fig. 6 the excess pore pressure ratio at WLA is plotted versus peak shear strain, calculated from double integration of the acceleration observations at 5.5 and 2.5 meter depths (Fig. 2) for the events from the Brawley swarm. The shear strain can be approximated to be at 4 meters depth, the mid-point between the two sensors, when double integrating to displacement, and dividing the difference by the distance between the sensors. The excess pore pressure observations in Fig. 6 are from the sensor 63 (Fig 2.) at 3.5 meters depth. Also included in Fig. 6 are three other events, including the M7.2 El Mayor earthquake, ~100 km from the WLA site and two events from the 2005 Obsidian Buttes swarm.

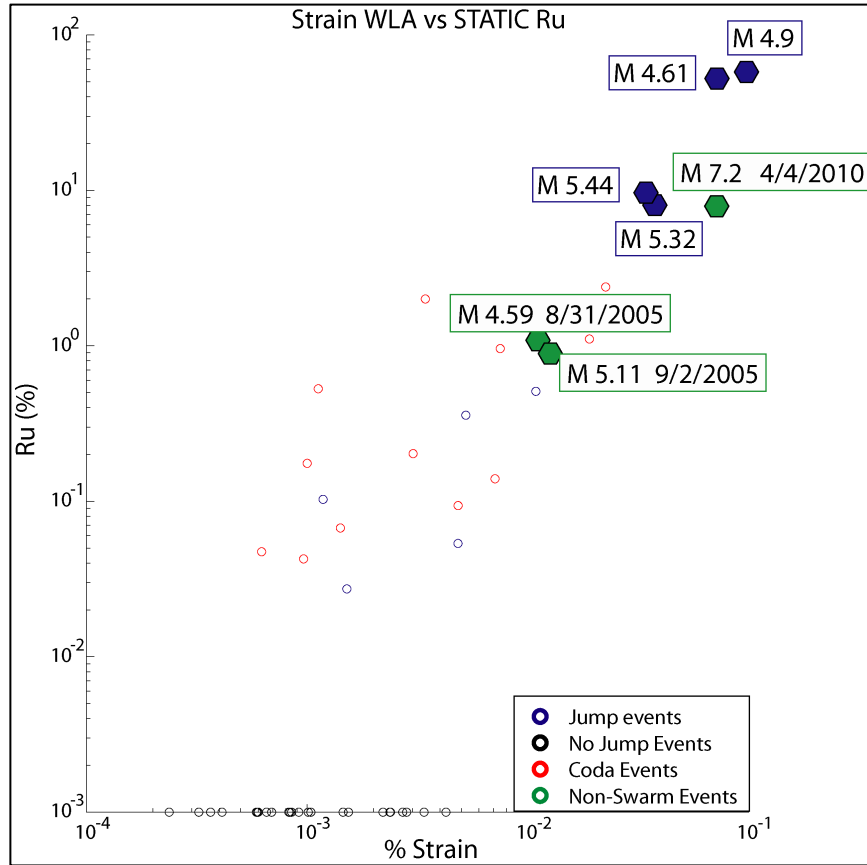


Figure 6. Excess pore pressure ratio vs. % strain.

The largest strain levels reach $\sim 1.8 \times 10^{-3}$ or $\sim 0.2\%$ strain for the 27 August 2012 M4.9 Brawley Swarm event that produced over 60% R_u excess pore pressure ratio. For this event, we had ground motions of ~ 15 cm/s in velocity. With a V_s in the liquefiable layer of ~ 150 m/s or 15000 cm/s we have a proxy strain using V/V_s of 15/15000 or 0.001 strain or 0.1% strain, slightly larger if you use the reduced velocity of ~ 100 m/s during strong shaking. These agree quite well with the measured strain using the double integrated acceleration records. In terms of the level of shear strain where you start to generate excess pore pressure, at WLA this threshold strain is approximately $10^{-3}\%$ strain, with a slight indication that it can happen at lower strain when looking at coda events where the soil has already softened. Fig. 6 also shows that some events above $1 \times 10^{-3}\%$ strain don't cause excess pore pressure generation, but once you get to $5 \times 10^{-3}\%$ strain, excess pore pressure is always generated. In terms of surface PGA at the WLA site, once you get above 50 cm/s², you always see some excess pore pressure generation. This can be seen in Fig. 7 where we plot % strain vs. PGA for the same data set.

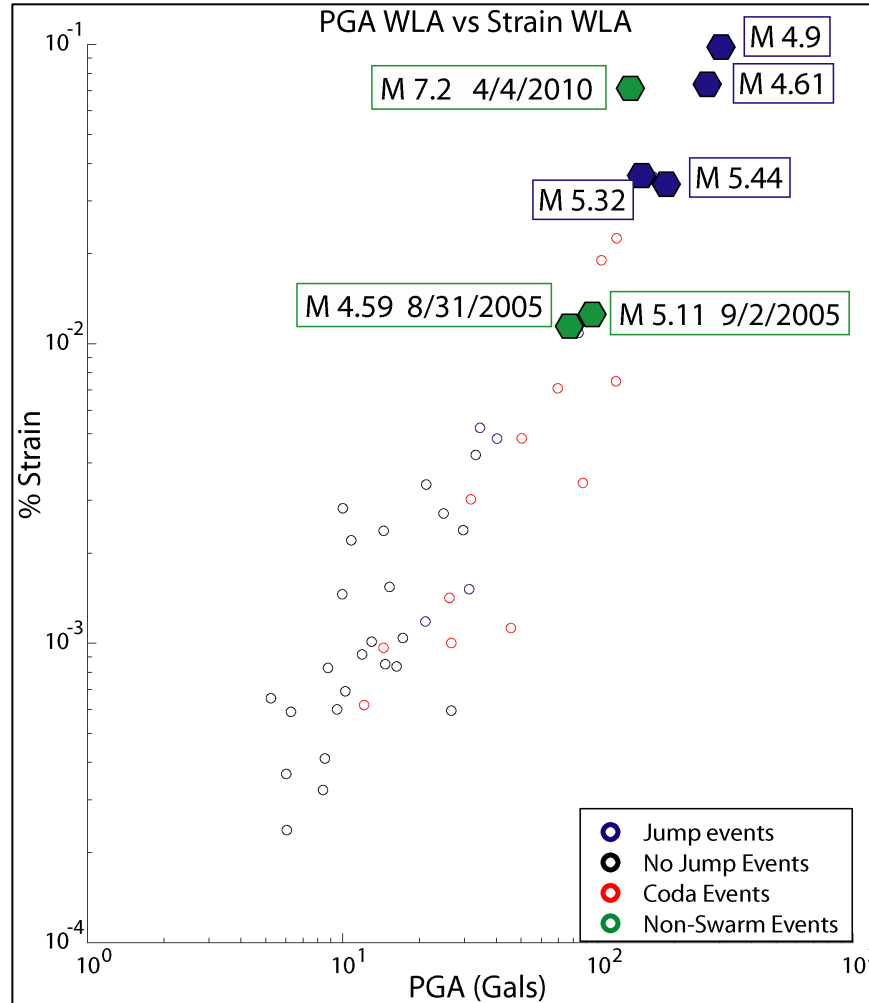


Figure 7. Percent strain vs. PGA.

Conclusions

Over the last decade, local and regional seismic activity, including multiple extremely active earthquake swarms, have produced a valuable new data set providing a unique opportunity to observe site response and the evolution of pore pressure generation with time throughout the liquefiable layer at an unprecedented level of detail. These new observations of pore pressure and acceleration with depth are providing *in situ* empirical evidence documenting the range of ground motion levels at which the onset of nonlinear behavior and excess pore pressure begins, augmenting previous case history data, and laboratory data from cyclic tri-axial and centrifuge testing.

Nonlinear soil behavior associated with the larger events in this swarm is analyzed in terms of changes in travel times (decrease in shear wave velocity) between accelerometers in the array for the largest ground motions, as well as a reduction in high frequency amplification for these events. The location of accelerometers at the surface and at five additional depths provides the opportunity to examine the contribution of the various layers to the overall site response.

Analysis of data during the largest excitation at the WLA site show that the nonlinear soil behavior occurs both near the surface and even at depths below 30 meters. The soil is observed to recover its pre-event low-strain velocities quickly following these larger events that occur during the swarms.

At WLA, excess pore pressure generation begins at PGA's of $\sim 50 \text{ cm/s}^2$ and $\sim 5 \times 10^{-3} \%$ strain levels. The largest static pore pressure increases observed in the "NEES" decade of monitoring were generated by four events at the WLA site, ranging in magnitude from 4.6 to 5.4 and all at distances less than 10km from the site. The largest peak horizontal acceleration of ~ 325 gals was generated by a M4.9 event. This event generated ~ 20 kPa of excess pore pressure on multiple transducers, with a pore pressure ratio R_u of $\sim 60\%$ near the top of the liquefiable layer. Using displacements calculated from the accelerometers above and below the liquefiable layer, peak strain levels reached as high as 0.18 % strain. During the Brawley Swarm events, which did not completely liquefy the site, the excess pore pressure can be seen migrating from the top of the layer towards the bottom in the continuous time history data, as well as dissipation that can take hours, highlighting the importance of continuous monitoring instead of triggered.

Acknowledgments

The author acknowledges the contributions of Scott Swain, Paul Hegarty, Les Youd, Robert Nigbor, Rob Steller, and Rod Merrill in the construction, maintenance, and operations of the field sites. The GVDA and WLA sites are currently operated under contract with the National Science Foundation as part of the George E. Brown Jr., Network for Earthquake engineering Simulation, award number CMMI-0927178. Without the support and cooperation of the Lake Hemet Municipal Water District and the California Department of Fish and Game, the monitoring at the GVDA and WLA sites would not be possible.

References

1. Steidl, J.H., Instrumented Geotechnical Sites: Current and future trends, *Proceedings of the 4th International Conference on Earthquake Geotechnical Engineering*, June 25-28, 2007, Paper No. W1-1009, p.234-245, Aristotle University of Thessaloniki, Greece.
2. Youd, T.L., J. H. Steidl, and R. L. Nigbor, Lessons learned and need for instrumented liquefaction sites, *Soil Dynamics and Earthquake Engineering*, 2004; vol. **24**, Issues 9-10, p 639-646.
3. Youd, T. L., J. H. Steidl, and R. A. Steller, Instrumentation of the Wildlife Liquefaction Array, K.D. Pitilakis (ed.), *Earthquake Geotechnical Engineering*, 2007; Paper No. 1251, Springer.
4. Steidl, J. H., and S. Seale, Observations and analysis of ground motion and pore pressure at the NEES instrumented geotechnical field sites, *Proceedings of the 5th International Conference on Recent Advances in Geotechnical Earthquake Engineering and Soil Dynamics, May 24-29, San Diego, CA*, 2010; paper No. 133b, ISBN-887009-15-9.
5. Steidl, J.H., R. Gee, S. Seale, and P. Hegarty, Recent enhancements to the NEES@UCSB permanently instrumented field sites, *Proceedings of the 15th World Conference on Earthquake Engineering*, September 24-28, 2012, Lisbon, Portugal, paper No. 4275.
6. Holzer, T. L., T. L. Youd, and T. C. Hanks, Dynamics of liquefaction during the 1897 Superstition Hills, California, *Earthquake, Science* 1989; **244** (4900), 56-59.
7. Zeghal, M. and A. W. Elgamel, Analysis of Site Liquefaction Using Earthquake Records, *Jour. Geotech. Eng.*

1994; **120** (6), 996-1017.

8. Holzer, T. L. and T. L. Youd, Liquefaction, Ground Oscillation, and Soil Deformation at the Wildlife Array, California, *Bull. Seism. Soc. Am.* 2007; **97** (3), 961 – 976.
9. Steidl, J. H., R. L. Nigbor and T. L. Youd, Observations of *in situ* Soil Behavior and Soil-Foundation-Structure Interaction at the George E. Brown, Jr., Network for Earthquake Engineering Simulation (NEES) Permanently Instrumented Field Sites, *Proc. Fourteenth World Conf. Earthquake Engineering*, October 12-17, 2008; Paper S16-01-14, Beijing, China.
10. Hauksson, E., J. Stock, R. Bilham, M. Boese, X. Chen, E. j. Fielding, J. Galetzka, K. W. Hudnut, K. Hutton, L. M. Jones, H. Kanamori, P. Shearer, J. H. Steidl, J. Treiman, S. Wei, and W. Yang, Report on the August 2012 Brawley Earthquake Swarm in Imperial Valley, Southern California, *Seismological Research Letters*, 2013; **84** (2), 177-189.
11. Idriss, I.M., and Boulanger, R.W., Soil Liquefaction during Earthquakes, *Monograph MNO-12*, 2008, Earthquake Engineering Research Institute. Oakland, CA.